Qubit-environment negativity versus fidelity of conditional environmental states for a nitrogen-vacancy-center spin qubit interacting with a nuclear environment

Małgorzata Strzałka,[1] Damian Kwiatkowski,[2] Łukasz Cywiński,[2] and Katarzyna Roszak[1]
[1]Department of Theoretical Physics, Wrocław University of Technology, 50-370 Wrocław, Poland
[2]Institute of Physics, Polish Academy of Sciences, 02-668 Warsaw, Poland

(Received 28 November 2019; revised 8 May 2020; accepted 11 September 2020; published 8 October 2020)

We study the evolution of qubit-environment entanglement, quantified using negativity, for nitrogen-vacancy-center spin qubits interacting with an environment of partially polarized nuclear spins in the diamond lattice. We compare it with the evolution of the fidelity of environmental states conditional on the pointer states of the qubit, which can serve as a tool to distinguish between entangling and nonentangling decoherence in the pure-dephasing scenario considered here. The two quantities show remarkable agreement during the evolution in a wide range of system parameters, leading to the conclusion that the amount of entanglement generated between the qubit and the environment is likely to be proportional to the trace that the joint evolution leaves on the environment.

DOI: 10.1103/PhysRevA.102.042602

I. INTRODUCTION

The study of system-environment entanglement or even qubit-environment entanglement is seriously limited due to large sizes of the studied environments, which translates into few entanglement measures being available on the level of density matrix considerations. This would not be a problem if the joint system-environment state was pure, but in most realistic scenarios the initial state of the environment is far from pure, except for extremely low temperatures. In fact, the only measure which can serve to quantify entanglement between two systems of any size which can be calculated directly from the joint density matrix is negativity [1,2] (or closely related logarithmic negativity [3]), which nevertheless requires diagonalization of a matrix of the same size as the joint system's Hilbert space. Negativity has its limitations, since there exist entangled states which are not detected by it [4,5], but it is the best available tool if the two potentially entangled systems are larger than a qubit and a qutrit and the purity of the system is less than one. All other measures require some form of minimization over possible representations of the states in different bases, which becomes highly cumbersome with growing system size [6–13].

Recently, relatively straightforward methods for detecting system-environment [14] and qubit-environment [15] entanglement have been found for a scenario in which the reduced state of the system undergoes pure dephasing in the basis of pointer states [16,17], which is singled out by the interaction itself. The main result of these papers was that the generation of system-environment entanglement during decoherence of the system occurs if the environment interacting with the system in distinct pointer states (the conditional states of environment) evolves into distinct states. Let us note that this is not only a canonical example of decoherence, in which the importance of establishment system-environment correlation for decoherence is particularly transparent [17,18], but it also describes the dominant decoherence mechanism for almost all the solid-state-based qubits [19–33] and also for trapped ions [34,35].

The problem of the method is that it does not quantify the amount of entanglement, instead answering the question if system-environment entanglement is present at a given time after initialization of the system or qubit in a pure state. As there are no limitations on the initial state of the environment, which is likely to be mixed, the whole system is initially impure, and pure dephasing can occur either while being accompanied by entanglement generation or due to completely separable system-environment evolutions [14,15,36–38]. This is in stark contrast to pure-state system-environment evolutions, for which pure dephasing is irrefutably linked with the buildup of entanglement with the environment [17,39]. The results of Refs [14,15] show that system-environment entanglement leaves a detectable trace on the environment, while it is impossible to distinguish entangling from nonentangling evolutions by straightforward measurements of system pure dephasing. More involved schemes for the detection of qubit-environment entanglement by operations and measurements on only the qubit subsystem have been recently proposed [40,41]. Both detection of entanglement by measurement only on the environment and detection of entanglement via operations on the qubit are possible because the problem is restricted to a special class of Hamiltonians, hence there is no contradiction with the popular theorem on the impossibility of local detection of entanglement.

The evolution of a qubit and its environment is not accompanied by entanglement generation if and only if the evolution of the states of the environment conditional on the pointer states of the qubit is the same at all times (if this occurs only at isolated points of time, then there is no entanglement only at these times) [15],

$$\hat{R}_{00}(t) = \hat{R}_{11}(t), \tag{1}$$

where said conditional states are denoted by $\hat{R}_{ii}(t)$, with $i = 0$ and 1, and they correspond to the state the environment would be in at time t if the qubit were initialized in pointer state $|i\rangle$ at the initial time. Hence if the qubit is initialized in a superposition state, $a|0\rangle + b|1\rangle$, the state of the environment at time t, obtained by tracing out the qubit from the full qubit-environment density matrix, is given by

$$\hat{R}(t) = |a|^2\hat{R}_{00}(t) + |b|^2\hat{R}_{11}(t). \tag{2}$$

In the case where there is no qubit-environment entanglement, this state is the same regardless of the initial qubit superposition and is equal to the state the environment would evolve to under the influence of the qubit in one of its pointer states. When entanglement with the environment is generated, the situation is qualitatively different, and the state of the environment depends on the probability of finding the qubit in either pointer state. Therefore we can talk about a trace left by joint qubit-environment evolution on the environment which is present only for entangling evolutions.

Here, we make a first step towards a measure of qubit-environment entanglement designed to quantify the amount of entanglement generated during evolutions of the pure-dephasing type. To this end, we test if the magnitude of the trace left by entangling evolutions on the state of the environment is proportional to the amount of actual entanglement generated on a realistically modeled nitrogen-vacancy (NV) center in diamond spin qubit interacting with a nuclear spin environment [33]. The choice of test system is based both on its experimental relevance [42–47] and on the wide variety of test scenarios it provides. As the NV center has effectively spin $S = 1$, the spin states form a qutrit, but the uneven level spacing between the different spin states allows for any two levels out of three to be singled out as the qubit under study. Furthermore, this type of spin qubit interacts strongly only with nuclei of spinful carbon isotopes ^{13}C, which are few within the diamond crystal lattice, and both their number and locations vary, which leads to different evolutions for different realizations of the environment of the qubit. The whole qubit-environment Hilbert space is therefore small enough to allow for effective diagonalization of matrices within it, which is necessary to find the evolution of negativity.

We test a number of qubit-environment evolutions driven by different interaction Hamiltonians, all within the NV-center spin qubit model with five randomly placed and partially spin-polarized relevant environmental nuclei. Results for other realizations of the environment are given in the Supplemental Material [48]. We find a remarkable agreement between the time evolution of the entanglement measure negativity and the fidelity between the states of the environment conditional on the qubit pointer states. Furthermore we find that this agreement is also present for evolutions which cannot be detected by the qubit-based schemes of Refs. [40,41]. We conjecture that the effect is of a more general nature, and that said, fidelity could be the basis of an entanglement measure designed specifically for pure-dephasing evolutions.

The paper is organized as follows. We introduce the NV-center qubit and its environment in Sec. II. In Sec. III we provide the definitions necessary to calculate qubit-environment negativity and show that the existence of unpolarized environmental spins does not influence its evolution. In Sec. IV we discuss the correlation between entanglement generation in pure-dephasing scenarios, and the difference between conditional evolution of the environment while using the fidelity to quantify this difference. Similarly to the section before, we also show that the existence of unpolarized environmental spins does not influence the evolution of the fidelity. Results obtained for realistically modeled spin qubits with randomly chosen environments are presented and discussed in Sec. V, while Sec. VI contains concluding remarks.

II. NV CENTER INTERACTING WITH A PARTIALLY POLARIZED NUCLEAR ENVIRONMENT

Our test system consists of a spin qubit defined on an NV center in diamond interacting with an environment of nuclear spins of the spinful carbon isotope ^{13}C. As most of the diamond crystal lattice consists of spinless carbon nuclei, the relevant (for decoherence) atoms of the environment are few and randomly located. This is of use for testing of the correlation between generated entanglement and the magnitude of the trace that entangling evolutions leave on the conditional states of the environment (how strongly the conditional states of the environment are affected by entangling evolution), since the resulting system-environment evolutions vary depending on the choice of qubit, as well as on the locations of the relevant nuclei and their number.

The low-energy states of the NV center constitute an effective electronic spin $S = 1$, so we are dealing with a qutrit defined on the $m = -1$, 0, and 1 levels, subsequently labeled as $|-1\rangle$, $|0\rangle$, and $|1\rangle$. This is subjected to a zero-field splitting, $\Delta(S^z)^2$, with the direction of the z axis determined by the geometry of the center, so the presence of a magnetic field along the z axis leads to a splitting of the $m_s = \pm 1$ levels and an uneven level spacing between all the levels. This allows for any two-level subspace to be used as a qubit controlled by microwave electromagnetic fields. We choose two out of the three possible qubits for our study, one is the most widely employed qubit based on the $m = 0$ and 1 levels, and the other is based on the $m = -1$ and 1 levels.

The large value of the zero-field splitting, $\Delta = 2.87$ GHz, and a large ratio of electronic and nuclear gyromagnetic factors lead to the suppression of transitions between the qutrit states mediated by the environment, hence the system can be described as one which undergoes only a pure-dephasing type of interaction [49]. Additionally, the $|0\rangle$ state is decoupled from the environment, so the qutrit-environment Hamiltonian is of the form

$$\begin{aligned}\hat{H} = &(\Delta + \gamma_e B_z)|-1\rangle\langle -1| + (\Delta - \gamma_e B_z)|1\rangle\langle 1| + \hat{H}_E \\ &- |-1\rangle\langle -1| \otimes \hat{V} + |1\rangle\langle 1| \otimes \hat{V}.\end{aligned} \tag{3}$$

The first two terms in the Hamiltonian describe the free evolution of the qutrit. The energies of states $|\pm 1\rangle$ depend on the zero-field splitting symmetrically and asymmetrically on a magnetic-field-dependent term, where $\gamma_e = 28.08$ MHz/T is the electron gyromagnetic ratio. This part of the Hamiltonian commutes with all other terms in Eq. (3) and the resulting evolution can therefore be eliminated from the joint system-environment evolution via a unitary operation performed solely on the qutrit (by moving to a rotation frame with respect to the qubit). The consequence of this is that this part has no bearing on either the generation of entanglement or on its magnitude. It will also play no part in the conditional evolution of the environment.

The second term in the Hamiltonian describes the free evolution of environmental spins,

$$\hat{H}_E = \sum_k \gamma_n B_z \hat{I}_k^z, \tag{4}$$

where k labels the spins, $\gamma_n = 10.71$ MHz/T is the gyromagnetic ratio for ^{13}C nuclei, and $\hat{I}_k^z$ is the operator of the z component of nuclear spin k. A term describing the internuclear magnetic dipolar interactions has been omitted, since the free evolution decoherence process occurs on timescales much shorter than those of the nuclear dynamics due to said interactions (in contrast to coherence observed in spin echo experiments [33,49]).

The last term in Eq. (3) describes the hyperfine interaction between the spin qubit and its nuclear spin environment. It is given by

$$\hat{V} = \sum_k \sum_{j\in(x,y,z)} \mathbb{A}_k^{z,j} \hat{I}_k^j. \tag{5}$$

If we omit the Fermi contact interaction [50] which is related to the nonzero probability of finding an electron bound to the NV center on the location of a given nucleus, and only take the dipolar coupling into account, the coupling constants present in Eq. (5) are given by

$$\mathbb{A}_k^{z,j} = \frac{\mu_0}{4\pi}\frac{\gamma_e\gamma_n}{r_k^3}\left(1 - \frac{3(\mathbf{r}_k\cdot\hat{\mathbf{j}})(\mathbf{r}_k\cdot\hat{\mathbf{z}})}{r_k^2}\right). \tag{6}$$

Here, μ_0 is the magnetic permeability of the vacuum, $\mathbf{r}_k$ is a displacement vector between the kth nucleus and the qubit and $\hat{\mathbf{j}} = \hat{\mathbf{x}}$, $\hat{\mathbf{y}}$, and $\hat{\mathbf{z}}$ denote versors corresponding to three distinct directions.

Note that the free evolution of the environment and the interaction term do not commute for nonzero magnetic fields; therefore the free evolution cannot be eliminated via a local unitary transformation and can take part in the generation of qubit-environment entanglement, regardless of the qubit of choice. Hence, the evolution operator for the qutrit and the environment (without the irrelevant free evolution of the qutrit) is given by

$$\hat{U}(t) = \sum_{m=-1}^{1} |m\rangle\langle m| \otimes \hat{w}_m(t), \tag{7}$$

with

$$\hat{w}_{-1}(t) = e^{-\frac{i}{\hbar}(\hat{H}_E - \hat{V})t}, \tag{8a}$$

$$\hat{w}_0(t) = e^{-\frac{i}{\hbar}\hat{H}_E t}, \tag{8b}$$

$$\hat{w}_1(t) = e^{-\frac{i}{\hbar}(\hat{H}_E + \hat{V})t}. \tag{8c}$$

Note that since both $\hat{H}_E$ and $\hat{V}$ can be written as sums over environmental spins k, each conditional evolution operator of the environment $\hat{w}_i(t)$ can be written in product form with respect to said spins for any instance of time t,

$$\hat{w}_i(t) = \bigotimes_k \hat{w}_i^k(t). \tag{9}$$

In the following we consider an initial state which is a product of a pure state of the qutrit within one of the two chosen qubit subspaces, $|\psi\rangle = a|0\rangle + b|1\rangle$ or $|\psi\rangle = a|-1\rangle + b|1\rangle$, and a partially polarized state of the nuclear environment, $\hat{R}(0)$, which is mixed,

$$\hat{\sigma}(0) = |\psi\rangle\langle\psi| \otimes \hat{R}(0). \tag{10}$$

The Hamiltonian (3) does not contain any terms which allow for transitions between different qutrit pointer states $|m\rangle$, so effectively the evolution of such an initial state is governed only by the terms in the Hamiltonian which contain the relevant qubit states, so either $|0\rangle$ and $|1\rangle$ or $|-1\rangle$ and $|1\rangle$. We assume that $\hat{R}(0)$ does not contain any correlations between the nuclei, so $\hat{R}(0) = \bigotimes_k \hat{\rho}_k(0)$, where $\hat{\rho}_k(0)$ is the density matrix of kth nucleus, given in the case of spin-1/2 nuclei by

$$\hat{\rho}_k(0) = \frac{1}{2}(\mathbb{1} + 2p_k\hat{I}_k^z), \tag{11}$$

where $p_k \in [-1, 1]$ is the polarization of the kth nucleus. Without dynamic nuclear polarization, $p_k = 0$ for all k, the density operator of the environment at low fields is $\hat{R}(0) \propto \mathbb{1}$, and according to the results of Ref. [15] no qubit-environment entanglement forms throughout the evolution. Since such nuclear polarization of the environment for an NV center has been recently mastered [51–59], the assumption of the specially prepared initial state of the environment is reasonable. In Sec. V we assume that the polarizations of each environmental nucleus are the same, so $p_k = p$ for all k, because in Secs. III and IV we show that additional interaction with any unpolarized environmental spins has no bearing on either the evolution of the negativity or the evolution of the fidelity between conditional states of the environment for the product initial state of the environment. This is relevant for the studied system, since dynamical nuclear polarization makes only some of the relevant environmental spins polarized. Note that the initially unpolarized environmental spins contribute to decoherence, even though they do not entangle with the qubit.

Since both the initial state and the evolution operator are known, we can write the time-evolved qubit-environment density matrix in the form

$$\tilde{\sigma}(t) = \begin{pmatrix} |a|^2\hat{R}_{nn}(t) & ab^*\hat{R}_{n1}(t) \\ a^*b\hat{R}_{1n}(t) & |b|^2\hat{R}_{11}(t) \end{pmatrix}, \tag{12}$$

with $n = -1$ and 0 depending on the choice of the qubit. Here the environmental operators $\hat{R}_{ij}(t)$ are given by

$$\hat{R}_{ij}(t) = \hat{w}_i(t)\hat{R}(0)\hat{w}_j^\dagger(t). \tag{13}$$

Since both the initial state of the environment and its conditional evolution operators (8) can always be written in product form, all matrices (13) can also be written in product form with respect to different spins of the environment at all times,

$$\hat{R}_{ij}(t) = \bigotimes_k \hat{\rho}_k^{ij}(t), \tag{14}$$

with

$$\hat{\rho}_k^{ij}(t) = \hat{w}_i^k(t)\hat{\rho}_k(0)\hat{w}_j^{k\dagger}(t). \quad (15)$$

III. NEGATIVITY—AN ENTANGLEMENT MEASURE APPLICABLE FOR LARGE BIPARTITE SYSTEMS

For large bipartite systems, such as the qubit and the environment (where the latter is larger) studied here, the choice of entanglement measures which can be computed is very limited. It comes down in fact practically to the choice between negativity [1,2] or logarithmic negativity [3]. Both measures are closely related and are based on the positive partial transpose (PPT) criterion of separability [60,61]. The criterion and therefore also the measures do not detect a certain type of entangled states called bound entangled states [4,5], but in the studied scenario, namely in the case of an initially pure-state qubit, bound entanglement never forms [15,62]. Therefore in what follows, negativity (and logarithmic negativity) signifies separability if and only if the joint qubit and environment state is really separable.

We choose to employ plain negativity, which is defined as the absolute sum of the negative eigenvalues of the density matrix of the whole system after a partial transposition with respect to one of the two potentially entangled subsystems and can be written as

$$N(\hat{\sigma}) = \sum_i \frac{|\lambda_i| - \lambda_i}{2}, \quad (16)$$

where λ_i denote all eigenvalues of the density matrix after partial transposition, $\hat{\sigma}^{\Gamma_A}$. Obviously the positive eigenvalues cancel out in Eq. (16) while only negative eigenvalues are left. Negativity does not depend on the system with respect to which partial transposition is performed, $A = Q$ and E.

We calculate negativity at each instance of time by first performing partial transposition with respect to the qubit on the time-evolved qubit-environment density matrix (12),

$$\tilde{\sigma}^{\Gamma_Q}(t) = \begin{pmatrix} |a|^2\hat{R}_{nn}(t) & a^*b\hat{R}_{1n}(t) \\ ab^*\hat{R}_{n1}(t) & |b|^2\hat{R}_{11}(t) \end{pmatrix}, \quad (17)$$

and then finding the eigevalues of the matrix obtained in this way.

At this point we can show that since all the environmental operators $\hat{R}_{1n}(t)$ retain their product form throughout the evolution (14), the presence of unpolarized environmental spins will not change the amount of entanglement as described by negativity, even though they do contribute to decoherence. To this end, let us divide the environment into a part composed of polarized nuclear spins, for which the initial state of each spin is given by Eq. (11), and a part composed of unpolarized spins, for which the initial state of each state is proportional to a unit matrix of appropriate dimension (which for spin 1/2 is obviously equal to 2). We denote the joint initial state of the polarized nuclei as $\hat{R}^{\mathrm{p}}(0)$ and that of the unpolarized nuclei as $\hat{R}^{\mathrm{np}}(0) = \frac{1}{M}\mathbb{I}_M$, and correspondingly the conditional evolution operators acting on the two parts of the environment as $\hat{w}_i^{\mathrm{p}}(t)$ and $\hat{w}_i^{\mathrm{np}}(t)$. Hence at all times we have

$$\hat{R}_{ij}(t) = \hat{R}_{ij}^{\mathrm{p}}(t) \otimes \hat{R}_{ij}^{\mathrm{np}}(t), \quad (18)$$

and we can write the qubit-environment density matrix after partial transposition (17) with

$$\hat{R}_{nn}(t) = \hat{R}_{nn}^{\mathrm{p}}(t) \otimes \mathbb{I}_M, \quad (19a)$$

$$\hat{R}_{11}(t) = \hat{R}_{11}^{\mathrm{p}}(t) \otimes \mathbb{I}_M, \quad (19b)$$

$$\hat{R}_{1n}(t) = \hat{R}_{1n}^{\mathrm{p}}(t) \otimes \hat{w}_1^{np}(t)\hat{w}_n^{\mathrm{np}\dagger}(t), \quad (19c)$$

$$\hat{R}_{n1}(t) = \hat{R}_{n1}^{\mathrm{p}}(t) \otimes \hat{w}_n^{np}(t)\hat{w}_1^{\mathrm{np}\dagger}(t), \quad (19d)$$

where $\hat{R}_{ij}^{\mathrm{p/np}}(t)$ is obtained following Eq. (13). Since $\hat{w}_1^{\mathrm{np}}(t)\hat{w}_n^{\mathrm{np}\dagger}(t)$ can be diagonalized, and the unit matrix which is defined on the same subspace retains the same form in any basis, the whole matrix (17) can be written as

$$\tilde{\sigma}^{\Gamma_Q}(t) = \frac{1}{M}\sum_m \begin{pmatrix} |a|^2\hat{R}_{nn}^{\mathrm{p}}(t) & a^*b\hat{R}_{1n}^{\mathrm{p}}(t)e^{i\phi_m} \\ ab^*\hat{R}_{n1}^{\mathrm{p}}(t)e^{-i\phi_m} & |b|^2\hat{R}_{11}^{\mathrm{p}}(t) \end{pmatrix} \otimes |m\rangle\langle m|, \quad (20)$$

at any time t. Here $e^{i\phi_m}$ and $|m\rangle$ are eigenvalues and eigenvectors of the unitary matrix $\hat{w}_1^{\mathrm{np}}(t)\hat{w}_n^{\mathrm{np}\dagger}(t)$.

It is now important to note that the matrix (20) is in fact block diagonal and each block corresponds to a given vector $|m\rangle$. Hence, finding the eigenvalues of this matrix reduces to finding the eigenvalues of each matrix,

$$\tilde{\sigma}_m^{\Gamma_Q}(t) = \begin{pmatrix} |a|^2\hat{R}_{nn}^{\mathrm{p}}(t) & a^*b\hat{R}_{1n}^{\mathrm{p}}(t)e^{i\phi_m} \\ ab^*\hat{R}_{n1}^{\mathrm{p}}(t)e^{-i\phi_m} & |b|^2\hat{R}_{11}^{\mathrm{p}}(t) \end{pmatrix}, \quad (21)$$

and dividing them by M. Hence the value of negativity obtained by diagonalization of the matrix in Eq. (20) must be equal to the average value of negativities obtained from the matrices (21),

$$N[\hat{\sigma}(t)] = \frac{1}{M}\sum_m N[\tilde{\sigma}_m(t)]. \quad (22)$$

Additionally, all of the matrices (21) are identical to the matrices which would be obtained when describing the joint evolution of the qubit with the part of the environment which is polarized with the exception of the phase factors $e^{i\phi_m}$. A single of these phase factors can be introduced into such a density matrix by a local unitary operation in the qubit subspace. Since it is known from the properties of negativity that its value cannot be changed by local unitary operations, obviously $N[\tilde{\sigma}_m(t)] = N[\tilde{\sigma}_{m'}(t)]$ for all m and m', so the addition of unpolarized environments does not influence the amount of entanglement in the system.

IV. FIDELITY OF CONDITIONAL ENVIRONMENTAL STATES

As shown in Refs [14,15], the if and only if criterion of separability for pure-dephasing qubit-environment evolutions at time t can be written as

$$\hat{R}_{nn}(t) = \hat{R}_{11}(t), \quad (23)$$

where the density matrices of the environment conditional on the qubit being in either of its pointer states are given by Eq. (13). This means that there is no entanglement between the qubit and the environment at time t, for an initial state that involves a pure state superposition in the qubit subspace, if and only if the environment would be in the same state at time

t if the qubit would have been initialized in either of its pointer states.

We conjecture that the degree of how different the two conditional density matrices are is proportional to the amount of entanglement generated throughout the evolution. To quantify this difference we use the fidelity between $\hat{R}_{nn}(t)$ and $\hat{R}_{11}(t)$, which yields a number between 0 and 1, 1 meaning that the states are the same and 0 meaning that they have orthogonal supports. The definition of fidelity for two arbitrary density matrices (of the same dimensionality) $\hat{R}_{nn}$ and $\hat{R}_{11}$ is

$$F\left(\hat{R}_{nn}, \hat{R}_{11}\right) = \left[\mathrm{Tr}\left(\sqrt{\sqrt{\hat{R}_{nn}}\hat{R}_{11}\sqrt{\hat{R}_{nn}}}\right)\right]^2. \tag{24}$$

Contrarily to negativity, described in the previous section, the product form which is retained by the conditional density matrices of the environment throughout the evolution results in the numerical complexity of calculating the fidelity growing very slowly with increasing size of the environment. This is because

$$F\left(\bigotimes_k \hat{\rho}_k^{nn}, \bigotimes_k \hat{\rho}_k^{11}\right) = \prod_k F\left(\hat{\rho}_k^{nn}, \hat{\rho}_k^{11}\right). \tag{25}$$

As in the previous section, we now show that the presence of unpolarized environmental spins does not change the fidelity (24), but the proof in this case is much simpler. We start with dividing the environment into parts as before, and we obtain the product form which is retained between the conditional density matrices of the environment throughout the evolution as in Eq. (18),

$$\hat{R}_{ii}(t) = \hat{R}_{ii}^{\mathrm{p}}(t) \otimes \hat{R}_{ii}^{\mathrm{np}}(t). \tag{26}$$

Inserting this into Eq. (24) and using the property (25) yields

$$\begin{aligned} F\left(\hat{R}_{nn}, \hat{R}_{11}\right) &= F\left(\hat{R}_{nn}^{\mathrm{p}}(t), \hat{R}_{11}^{\mathrm{p}}(t)\right) F\left(\hat{R}_{nn}^{\mathrm{np}}(t), \hat{R}_{11}^{\mathrm{np}}(t)\right) \\ &= F\left(\hat{R}_{nn}^{\mathrm{p}}(t), \hat{R}_{11}^{\mathrm{p}}(t)\right), \end{aligned} \tag{27}$$

since

$$\hat{R}_{ii}^{\mathrm{np}}(t) = \hat{w}_i^{\mathrm{np}}(t)\frac{\mathbb{I}_M}{M}\hat{w}_i^{\mathrm{np}\dagger}(t) = \frac{\mathbb{I}_M}{M}, \tag{28}$$

regardless of the index i.

V. RESULTS

In the following we compare the evolution of negativity between one of the two chosen qubits and the environment and one-minus-fidelity between the conditional states of the environment, $1 - F[\hat{R}_{nn}(t), \hat{R}_{11}(t)]$, where $n = -1$ or 0 is specified by the choice of qubit. As the aim here is to study exemplary evolutions of the type found for NV-center qubits interacting with a nuclear environment, we use the same randomly chosen realization of the spin environment in all plots. They correspond to an environment composed of five initially partially polarized ^{13}C isotopes (nuclear spin 1/2) for which their randomly generated spatial arrangement determines the coupling constants (6). The distances of each environmental spin from the qubit and the coupling constants are given in Table I. Analogous sets of plots for other realizations of the environment are provided in the Supplemental Material [48].

TABLE I. Distances of each environmental spin from the NV-center qubit and the corresponding coupling constants for the realization of the environment used in Figs. 1–5.

k	r_k (nm)	$\mathbb{A}_k^{z,x}$ $(1/\mu s)$	$\mathbb{A}_k^{z,y}$ $(1/\mu s)$	$\mathbb{A}_k^{z,z}$ $(1/\mu s)$
1	0.563 961	0.492 352	0.511 667	−0.417 774
2	0.617 788	0	0	1.059 37
3	0.636 801	−0.093 878 9	0.069 687	−0.47416
4	0.667 287	0	−0.441 263	0.660531
5	0.667 287	−0.169 842	0.588 35	0.060 048 3

The evolution of twice the negativity between the $m = 0$ and 1 qubits and an environment is plotted for $B_z = 0$ and $B_z = 0.2$ T in Figs. 1 and 2, respectively, using dashed red lines. For the $m = -1$ and 1 qubits, analogous plots are found in Fig. 3 for $B_z = 0$ and in Fig. 4 for $B_z = 0.2$ T. The evolution of the one-minus-fidelity between the conditional states of the environment, $1 - F[\hat{R}_{nn}(t), \hat{R}_{11}(t)]$, is plotted in the same figures using solid blue lines, with $n = 0$ for Figs. 1 and 2 and with $n = -1$ for Figs. 3 and 4. The panels (a), (b), (c), and (d) in all figures correspond to growing initial polarization of the environment, with the most mixed environment (corresponding to $p = 0.1$, so not maximally mixed) in panels (a) and fully polarized environments in panels (d). All of the figures contain results for an initial equal superposition qubit state (the initial phase between the components of this superposition is irrelevant). Let us note that dephasing of the qubit, described in detail for an unpolarized environment in Ref. [49], is caused both by the few polarized nuclei in the close vicinity of the qubit and by the ∼100 unpolarized nuclei farther away. The typical timescale of this process is a few microseconds, so that the entanglement shown in Figs. 1–4 becomes significant on the timescale on which the qubit is already dephased. It is however important to note that this is a coincidence: the dephasing is mostly caused by

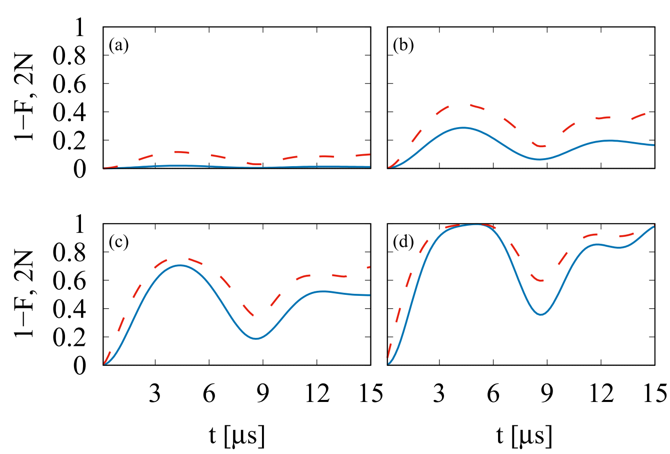

FIG. 1. Evolution of qubit-environment negativity (red dashed lines) and one-minus-fidelity between conditional environmental states (blue solid lines) for a qubit defined on $m = 0$ and $m = 1$ spin states and five environmental spins at random locations as a function of time for $B_z = 0.2$ T and different initial polarizations of the environment: (a) $p = 0.1$, (b) $p = 0.4$, (c) $p = 0.7$, and (d) $p = 1$.

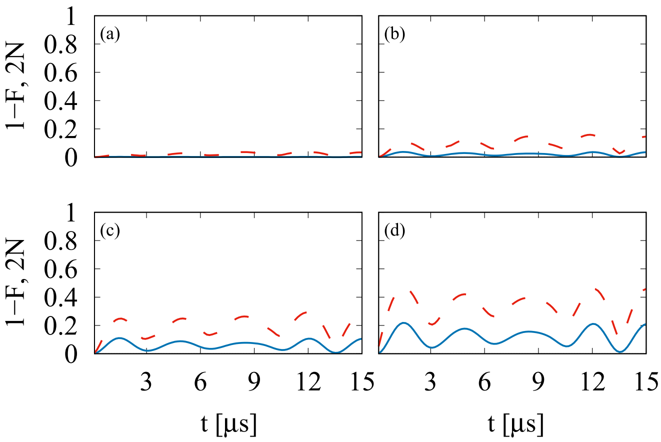

FIG. 2. Same as Fig. 1, but for $B_z = 0.2$ T.

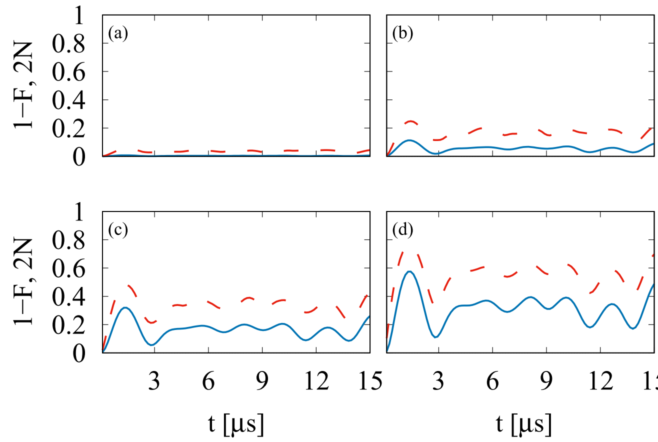

FIG. 4. Same as Fig. 3, but for $B_z = 0.2$ T.

the unpolarized environmental spins that do not participate in qubit-environment entanglement.

As should be expected [15], for a completely mixed environment, $p = 0$, qubit decoherence is not accompanied by the generation of entanglement regardless of the type of interaction with the environment, since the initial density matrix of the environment is proportional to unity and commutes with any possible environmental evolution operators [15]. This does not mean that the qubit does not experience decoherence and, in fact, the qubit becomes dephased during the evolution in all four of the studied situations with not polarized initial states of the environment.

For partially and fully polarized initial environmental states, generation of entanglement is observed regardless of the variant of the Hamiltonian under study. This has been predicted for the $m = 0$ and 1 qubits when $B_z \neq 0$, which has been used to exemplify the scheme for detection of qubit-environment entanglement via operations only on the qubit subsystem [40]. The procedure described there could also be used to predict the generation of qubit-environment entanglement for the $m = -1$ and 1 qubits and $B_z \neq 0$. This is because the condition for the procedure described in Ref. [40] to be able to detect qubit-environment entanglement is for the evolution operators on the environment conditional on the pointer state of the qubit (8) not to commute, so

$$[\hat{w}_n(t), \hat{w}_1(t)] \neq 0, \tag{29}$$

with $n = -1$ and 0 depending on the choice of qubit. This condition is met for $B_z \neq 0$, but not for $B_z = 0$ when $\hat{w}_{-1}(t) = \hat{w}_1^{\dagger}(t)$ and $\hat{w}_0(t) = \mathbb{I}$.

More interestingly, the evolution of the quantity $1 - F[\hat{R}_{nn}(t), \hat{R}_{11}(t)]$, which determines how different the two conditional states of the environment are at time t, resembles the evolution of the negativity very closely. In fact, $1 - F[\hat{R}_{nn}(t), \hat{R}_{11}(t)]$ grows when negativity grows, decreases when negativity decreases, and remains constant when negativity remains constant with very rare discrepancies. To exemplify this, in Fig. 5 we plot the time derivatives of both negativity and one-minus-fidelity corresponding to the evolutions in Fig. 1. It can be seen that the derivatives of both

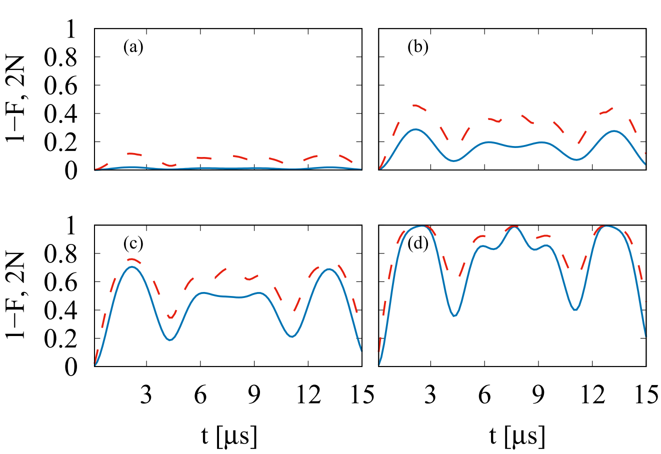

FIG. 3. Same as Fig. 1, but for a qubit defined on $m = -1$ and $m = 1$ spin states.

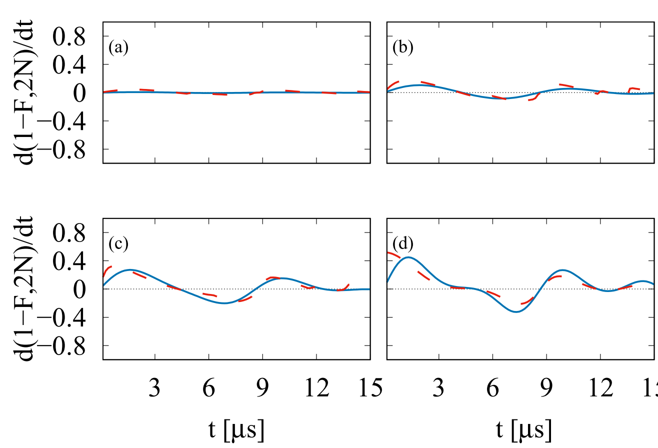

FIG. 5. Time-derivative of the evolution of qubit-environment negativity (red dashed lines) and one-minus-fidelity between conditional environmental states (blue solid lines) for a qubit defined on $m = 0$ and $m = 1$ spin states and five environmental spins at random locations as a function of time for zero magnetic field and different initial polarizations of the environment: (a) $p = 0.1$, (b) $p = 0.4$, (c) $p = 0.7$, and (d) $p = 1$. The figure corresponds to the evolutions in Fig. (1).

quantities are positive, negative, and equal to 0 at the same segments or points of time.

Figures analogous to Figs. 1–5 but corresponding to three different realizations of the environment are provided in the Supplemental Material [48]. They display the same qualitative and quantitative similarity in the evolution of negativity and one-minus-fidelity.

The close similarity between N and $1 - F$ is present in all four situations studied, which correspond to one physical scenario, but differ quite extensively, containing an asymmetric system-environment coupling (the $m = 0$ and 1 qubit) with ($B_z = 0$) and without ($B_z \neq 0$) commuting environmental and interaction parts of the Hamiltonian, as well as a coupling which is not asymmetric (the $m = -1$ and 1 qubit) again in two variants pertaining to the commutation of parts of the Hamiltonian. It is thus reasonable to assume that the close resemblance of the negativity and one-minus-fidelity evolutions is not accidental.

VI. CONCLUSION

We have studied four variations of an NV-center spin qubit interacting with an environment of nuclear spins, out of which a few are polarized. The interaction leads to pure dephasing of the qubit, caused by both polarized and unpolarized nuclei, and to creation of entanglement between the qubit and the few polarized nuclei. The variations are obtained by the choice of qubit under study (by choosing distinct pairs of levels of the NV-center qutrit we analyze two out of three possible qubits), which yields different effective interaction Hamiltonians, and by the application of the magnetic field or lack thereof. The latter facilitates the transition between commuting and noncommuting conditional evolution operators of the environment and is important from the point of view of detecting this type of entanglement.

We have first shown that the evolution of the entanglement measure negativity as well as the evolution of the fidelity between conditional states of the environment does not depend on the presence of initially unpolarized environmental spins. We have then compared the time evolution of the amount of entanglement between the qubit and the environment with the time evolution of one-minus-fidelity for an environment composed only of spins which were initially partially polarized. In all the studied situations the evolution of one-minus-fidelity resembled the evolution of negativity very closely.

We conjecture that the amount of entanglement with the environment generated during any evolution that leads to pure dephasing of the qubit for an initial product state of a pure qubit and environment is proportional to one-minus-fidelity between the states of the environment conditional on the qubit pointer states. This would mean that the amount of entanglement generated between the qubit and the environment is proportional to the trace that the joint evolution leaves on the environment. Hence, although it is not possible to distinguish between entangling and nonentangling evolutions by studying only qubit dephasing, it not only is possible to distinguish them by detecting the difference in environmental evolution linked to the different pointer states of the qubit but may also be possible to quantify the amount of entanglement in the qubit-environment system by studying the magnitude of this difference. We have shown this to be the case in quantitatively different situations which can be realized in NV-center spin qubits. The advantage is that, contrary to other measures of mixed-state entanglement, here we have a natural physical interpretation, which in fact is the same as for the pure state entanglement in pure-dephasing scenarios (namely, entanglement is proportional to how much the two conditional states of the environment differ from one another).

In fact, recently, it has been shown in Ref. [63] that one-minus-fidelity between the conditional density matrices of the environment is, after normalization with respect to the parameters of the initial superposition state of the qubit, an entanglement measure. All of the one-minus-fidelity plots show the evolution of entanglement quantified by the measure of Ref. [63], which would be obtained for an equal superposition initial qubit state.

The results presented here would be hard to reproduce experimentally because of the size of the environment, which hinders the reconstruction of the qubit-environment state through tomography. There exist proposals to measure the fidelity [64–66] and negativity [67–69] more directly, which could at least in principle be used to study these quantities in the case of the NV-center spin qubit and its environment. Another class of schemes, such as coarse-grained collective measurement [70–73], which rely on measurements of collective quantities of larger systems (such as magnetization) could be potentially used to experimentally distinguish between different states of the nuclear environment, but a careful analysis of how reliable such schemes would prove (and how to optimize the measurement for quantification of entanglement) is beyond the scope of this work.

ACKNOWLEDGMENT

This work was supported by funds from the Polish National Science Center (NCN), Grant No. 2015/19/B/ST3/03152.

[1] G. Vidal and R. F. Werner, Computable measure of entanglement, Phys. Rev. A **65**, 032314 (2002).

[2] J. Lee, M. Kim, Y. Park, and S. Lee, Partial teleportation of entanglement in a noisy environment, J. Mod. Opt. **47**, 2151 (2000).

[3] M. B. Plenio, Logarithmic Negativity: A Full Entanglement Monotone That is not Convex, Phys. Rev. Lett. **95**, 090503 (2005).

[4] P. Horodecki, Separability criterion and inseparable mixed states with positive partial transposition, Phys. Lett. A **232**, 333 (1997).

[5] M. Horodecki, P. Horodecki, and R. Horodecki, Mixed-State Entanglement and Distillation: Is there a "Bound" Entanglement in Nature? Phys. Rev. Lett. **80**, 5239 (1998).

[6] B. Kraus, J. I. Cirac, S. Karnas, and M. Lewenstein, Separability in $2 \times n$ composite quantum systems, Phys. Rev. A **61**, 062302 (2000).

[7] L. Gurvits, Classical deterministic complexity of Edmonds' problem and quantum entanglement, in *Proceedings of the Thirty-fifth Annual ACM Symposium on Theory of Computing*, STOC '03 (ACM Press, New York, 2003), pp. 10–19.

[8] F. Mintert, A. R. R. Carvalho, M. Kuś, and A. Buchleitner, Measures and dynamics of entangled states, Phys. Rep. **415**, 207 (2005).

[9] M. B. Plenio and S. Virmani, An introduction to entanglement measures, Quantum Inf. Comput. **7**, 1 (2007).

[10] L. M. Ioannou, Computational complexity of the quantum separability problem, Quantum Inf. Comput. **7**, 335 (2007).

[11] R. Horodecki, P. Horodecki, M. Horodecki, and K. Horodecki, Quantum entanglement, Rev. Mod. Phys. **81**, 865 (2009).

[12] Y. Huang, Computing quantum discord is NP-complete, New J. Phys. **16**, 033027 (2014).

[13] L. Aolita, F. de Melo, and L. Davidovich, Open-system dynamics of entanglement, Rep. Prog. Phys. **78**, 042001 (2015).

[14] K. Roszak, Criteria for system-environment entanglement generation for systems of any size in pure-dephasing evolutions, Phys. Rev. A **98**, 052344 (2018).

[15] K. Roszak and Ł. Cywiński, Characterization and measurement of qubit-environment-entanglement generation during pure dephasing, Phys. Rev. A **92**, 032310 (2015).

[16] W. H. Żurek, Pointer basis of quantum apparatus: Into what mixture does the wave packet collapse? Phys. Rev. D **24**, 1516 (1981).

[17] W. H. Żurek, Decoherence, einselection, and the quantum origins of the classical, Rev. Mod. Phys. **75**, 715 (2003).

[18] M. Schlosshauer, *Decoherence and the Quantum-to-Classical Transition* (Springer, Berlin, 2007).

[19] J. Medford, Ł. Cywiński, C. Barthel, C. M. Marcus, M. P. Hanson, and A. C. Gossard, Scaling of dynamical decoupling for spin qubits, Phys. Rev. Lett. **108**, 086802 (2012).

[20] E. Kawakami, T. Jullien, P. Scarlino, D. R. Ward, D. E. Savage, M. G. Lagally, V. V. Dobrovitski, M. Friesen, S. N. Coppersmith, M. A. Eriksson, and L. M. K. Vandersypen, Gate fidelity and coherence of an electron spin in an Si/SiGe quantum dot with micromagnet, Proc. Natl. Acad. Sci. USA **113**, 11738 (2016).

[21] P. Borri, W. Langbein, S. Schneider, U. Woggon, R. L. Sellin, D. Ouyang, and D. Bimberg, Ultralong Dephasing Time in InGaAs Quantum Dots, Phys. Rev. Lett. **87**, 157401 (2001).

[22] A. Vagov, V. M. Axt, T. Kuhn, W. Langbein, P. Borri, and U. Woggon, Nonmonotonous temperature dependence of the initial decoherence in quantum dots, Phys. Rev. B **70**, 201305(R) (2004).

[23] K. Roszak and P. Machnikowski, Complete disentanglement by partial pure dephasing, Phys. Rev. A **73**, 022313 (2006).

[24] E. Paladino, Y. M. Galperin, G. Falci, and B. L. Altshuler, $1/f$ noise: Implications for solid-state quantum information, Rev. Mod. Phys. **86**, 361 (2014).

[25] P. Szańkowski, G. Ramon, J. Krzywda, D. Kwiatkowski, and Ł. Cywiński, Environmental noise spectroscopy with qubits subjected to dynamical decoupling, J. Phys.: Condens. Matter **29**, 333001 (2017).

[26] W. M. Witzel and S. Das Sarma, Quantum theory for electron spin decoherence induced by nuclear spin dynamics in semiconductor quantum computer architectures: Spectral diffusion of localized electron spins in the nuclear solid-state environment, Phys. Rev. B **74**, 035322 (2006).

[27] W. Yao, R.-B. Liu, and L. J. Sham, Theory of electron spin decoherence by interacting nuclear spins in a quantum dot, Phys. Rev. B **74**, 195301 (2006).

[28] Ł. Cywiński, W. M. Witzel, and S. Das Sarma, Pure quantum dephasing of a solid-state electron spin qubit in a large nuclear spin bath coupled by long-range hyperfine-mediated interaction, Phys. Rev. B **79**, 245314 (2009).

[29] W. A. Coish, J. Fischer, and D. Loss, Free-induction decay and envelope modulations in a narrowed nuclear spin bath, Phys. Rev. B **81**, 165315 (2010).

[30] H. Bluhm, S. Foletti, I. Neder, M. Rudner, D. Mahalu, V. Umansky, and A. Yacoby, Long coherence of electron spins coupled to a nuclear spin bath, Nat. Phys. **7**, 109 (2010).

[31] W. Yang, W.-L. Ma, and R.-B. Liu, Quantum many-body theory for electron spin decoherence in nanoscale nuclear spin baths, Rep. Prog. Phys. **80**, 016001 (2017).

[32] F. K. Malinowski, F. Martins, P. D. Nissen, E. Barnes, Ł. Cywiński, M. S. Rudner, S. Fallahi, G. C. Gardner, M. J. Manfra, C. M. Marcus, and F. Kuemmeth, Notch filtering the nuclear environment of a spin qubit, Nat. Nanotechnol. **12**, 16 (2017).

[33] D. Kwiatkowski and Ł. Cywiński, Decoherence of two entangled spin qubits coupled to an interacting sparse nuclear spin bath: Application to nitrogen vacancy centers, Phys. Rev. B **98**, 155202 (2018).

[34] M. J. Biercuk, H. Uys, A. P. VanDevender, N. Shiga, W. M. Itano, and J. J. Bollinger, Optimized dynamical decoupling in a model quantum memory, Nature (London) **458**, 996 (2009).

[35] T. Monz, P. Schindler, J. T. Barreiro, M. Chwalla, D. Nigg, W. A. Coish, M. Harlander, W. Hänsel, M. Hennrich, and R. Blatt, 14-Qubit Entanglement: Creation and Coherence, Phys. Rev. Lett. **106**, 130506 (2011).

[36] J. Eisert and M. B. Plenio, Quantum and Classical Correlations in Quantum Brownian Motion, Phys. Rev. Lett. **89**, 137902 (2002).

[37] S. Hilt and E. Lutz, System-bath entanglement in quantum thermodynamics, Phys. Rev. A **79**, 010101(R) (2009).

[38] A. Pernice and W. T. Strunz, Decoherence and the nature of system-environment correlations, Phys. Rev. A **84**, 062121 (2011).

[39] K. Hornberger, Introduction to Decoherence Theory, in *Entanglement and Decoherence, Foundations and Modern Trends*, edited by A. Buchleitner, C. Viviescas, and M. Tiersch, Lecture Notes in Physics, Vol. 768 (Springer, Berlin, 2009), pp. 221–276.

[40] K. Roszak, D. Kwiatkowski, and Ł. Cywiński, How to detect qubit-environment entanglement generated during qubit dephasing, Phys. Rev. A **100**, 022318 (2019).

[41] B. Rzepkowski and K. Roszak, A scheme for direct detection of qubit-environment entanglement generated during qubit pure dephasing, arXiv:2002.10901.

[42] T. Staudacher, F. Shi, S. Pezzagna, J. Meijer, J. Du, C. A. Meriles, F. Reinhard, and J. Wrachtrup, Nuclear magnetic

resonance spectroscopy on a (5-nanometer)^3 sample volume, Science **339**, 561 (2013).

[43] S. J. DeVience, L. M. Pham, I. Lovchinsky, A. O. Sushkov, N. Bar-Gill, C. Belthangady, F. Casola, M. Corbett, H. Zhang, M. Lukin, H. Park, A. Yacoby, and R. L. Walsworth, Nanoscale NMR spectroscopy and imaging of multiple nuclear species, Nat. Nanotechnol. **10**, 129 (2015).

[44] T. Häberle, D. Schmid-Lorch, F. Reinhard, and J. Wrachtrup, Nanoscale nuclear magnetic imaging with chemical contrast, Nat. Nanotechnol. **10**, 125 (2015).

[45] I. Lovchinsky, A. O. Sushkov, E. Urbach, N. P. de Leon, S. Choi, K. D. Greve, R. Evans, R. Gertner, E. Bersin, C. Müller, L. McGuinness, F. Jelezko, R. L. Walsworth, H. Park, and M. D. Lukin, Nuclear magnetic resonance detection and spectroscopy of single proteins using quantum logic, Science **351**, 836 (2016).

[46] J. Wrachtrup and A. Finkler, Single spin magnetic resonance, J. Magn. Res. **269**, 225 (2016).

[47] C. L. Degen, F. Reinhard, and P. Cappellaro, Quantum sensing, Rev. Mod. Phys. **89**, 035002 (2017).

[48] See Supplemental Material at http://link.aps.org/supplemental/10.1103/PhysRevA.102.042602 for results for other realizations of the environment.

[49] N. Zhao, S.-W. Ho, and R.-B. Liu, Decoherence and dynamical decoupling control of nitrogen vacancy center electron spins in nuclear spin baths, Phys. Rev. B **85**, 115303 (2012).

[50] A. Gali, M. Fyta, and E. Kaxiras, *Ab initio* supercell calculations on nitrogen-vacancy center in diamond: Electronic structure and hyperfine tensors, Phys. Rev. B **77**, 155206 (2008).

[51] P. London, J. Scheuer, J. M. Cai, I. Schwarz, A. Retzker, M. B. Plenio, M. Katagiri, T. Teraji, S. Koizumi, J. Isoya, R. Fischer, L. P. McGuinness, B. Naydenov, and F. Jelezko, Detecting and Polarizing Nuclear Spins with Double Resonance on a Single Electron Spin, Phys. Rev. Lett. **111**, 067601 (2013).

[52] R. Fischer, C. O. Bretschneider, P. London, D. Budker, D. Gershoni, and L. Frydman, Bulk Nuclear Polarization Enhanced at Room Temperature by Optical Pumping, Phys. Rev. Lett. **111**, 057601 (2013).

[53] D. Pagliero, K. R. Koteswara Rao, P. R. Zangara, S. Dhomkar, H. H. Wong, A. Abril, N. Aslam, A. Parker, J. King, C. E. Avalos, A. Ajoy, J. Wrachtrup, A. Pines, and C. A. Meriles, Multispin-assisted optical pumping of bulk ^{13}C nuclear spin polarization in diamond, Phys. Rev. B **97**, 024422 (2018).

[54] R. Wunderlich, J. Kohlrautz, B. Abel, J. Haase, and J. Meijer, Optically induced cross relaxation via nitrogen-related defects for bulk diamond ^{13}C hyperpolarization, Phys. Rev. B **96**, 220407(R) (2017).

[55] G. A. Álvarez, C. O. Bretschneider, R. Fischer, P. London, H. Kanda, S. Onoda, J. Isoya, D. Gershoni, and L. Frydman, Local and bulk ^{13}C hyperpolarization in nitrogen-vacancy-centred diamonds at variable fields and orientations, Nat. Commun. **6**, 8456 (2015).

[56] J. P. King, K. Jeong, C. C. Vassiliou, C. S. Shin, R. H. Page, C. E. Avalos, H.-J. Wang, and A. Pines, Room-temperature *in situ* nuclear spin hyperpolarization from optically pumped nitrogen vacancy centres in diamond, Nat. Commun. **6**, 8965 (2015).

[57] J. Scheuer, I. Schwartz, S. Müller, Q. Chen, I. Dhand, M. B. Plenio, B. Naydenov, and F. Jelezko, Robust techniques for polarization and detection of nuclear spin ensembles, Phys. Rev. B **96**, 174436 (2017).

[58] F. Poggiali, P. Cappellaro, and N. Fabbri, Measurement of the excited-state transverse hyperfine coupling in NV centers via dynamic nuclear polarization, Phys. Rev. B **95**, 195308 (2017).

[59] Y. Hovav, B. Naydenov, F. Jelezko, and N. Bar-Gill, Low-Field Nuclear Polarization using Nitrogen Vacancy Centers in Diamonds, Phys. Rev. Lett. **120**, 060405 (2018).

[60] A. Peres, Separability Criterion for Density Matrices, Phys. Rev. Lett. **77**, 1413 (1996).

[61] M. Horodecki, P. Horodecki, and R. Horodecki, Separability of mixed states: Necessary and sufficient conditions, Phys. Lett. A **223**, 1 (1996).

[62] P. Horodecki, M. Lewenstein, G. Vidal, and I. Cirac, Operational criterion and constructive checks for the separability of low-rank density matrices, Phys. Rev. A **62**, 032310 (2000).

[63] K. Roszak, A measure of qubit environment entanglement for pure dephasing evolutions, Phys. Rev. Research (to be published), arXiv:1912.07317.

[64] A. J. Daley, H. Pichler, J. Schachenmayer, and P. Zoller, Measuring Entanglement Growth in Quench Dynamics of Bosons in an Optical Lattice, Phys. Rev. Lett. **109**, 020505 (2012).

[65] D. A. Abanin and E. Demler, Measuring Entanglement Entropy of a Generic Many-Body System with a Quantum Switch, Phys. Rev. Lett. **109**, 020504 (2012).

[66] L. Banchi, A. Bayat, and S. Bose, Entanglement entropy scaling in solid-state spin arrays via capacitance measurements, Phys. Rev. B **94**, 241117(R) (2016).

[67] H. A. Carteret, Noiseless Quantum Circuits for the Peres Separability Criterion, Phys. Rev. Lett. **94**, 040502 (2005).

[68] K. Bartkiewicz, P. Horodecki, K. Lemr, A. Miranowicz, and K. Życzkowski, Method for universal detection of two-photon polarization entanglement, Phys. Rev. A **91**, 032315 (2015).

[69] J. Gray, L. Banchi, A. Bayat, and S. Bose, Machine-Learning-Assisted Many-Body Entanglement Measurement, Phys. Rev. Lett. **121**, 150503 (2018).

[70] A. J. Leggett, Testing the limits of quantum mechanics: Motivation, state of play, prospects, J. Phys.: Condens. Matter **14**, R415 (2002).

[71] U. L. Andersen and J. S. Neergaard-Nielsen, Heralded generation of a micro-macro entangled state, Phys. Rev. A **88**, 022337 (2013).

[72] A. Lvovsky, R. Ghobadi, A. Chandra, A. S. Prasad, and C. Simon, Observation of micro-macro entanglement of light, Nat. Phys. **9**, 541 (2013).

[73] M. S. Mirkamali and D. G. Cory, Mesoscopic spin systems as quantum entanglers, Phys. Rev. A **101**, 032320 (2020).